



Contents lists available at ScienceDirect

Bioorganic & Medicinal Chemistry Letters

journal homepage: www.elsevier.com/locate/bmcl

Molecular hybridization yields triazole bronchodilators for the treatment of COPD



Lyn H. Jones^{a,*}, Jane Burrows^b, Neil Feeder^b, Paul Glossop^c, Kim James^c, Rhys M. Jones^d, Amy S. Kenyon^c, Sheena Patel^{e,f}, Dannielle F. Roberts^c, Matthew D. Selby^c, Ross S. Strang^c, Emilio F. Stuart^e, Michael A. Trevethick^e, Jessica Watson^e, Karen N. Wright^e, Nick Clarke^{e,g}

^a WorldWide Medicinal Chemistry, 610 Main Street, Cambridge, MA 02139, USA

^b Pharmaceutical Sciences, Pfizer, Ramsgate Road, Sandwich CT13 9NJ, UK

^c WorldWide Medicinal Chemistry, Pfizer, Ramsgate Road, Sandwich CT13 9NJ, UK

^d Pharmacokinetics, Dynamics and Metabolism, 610 Main Street, Cambridge, MA 02139, USA

^e Allergy and Respiratory Biology, Pfizer, Ramsgate Road, Sandwich CT13 9NJ, UK

^f CVMED Research Unit, Pfizer, Cambridge, MA 02139, USA

^g Inflammation and Immunology Research Unit, Pfizer, 610 Main Street, Cambridge, MA 02139, USA

ARTICLE INFO

Article history:

Received 1 August 2015

Revised 29 September 2015

Accepted 5 October 2015

Available online 8 October 2015

Keywords:

MABA

Inhalation by design

COPD

Bronchodilator

Bifunctional

ABSTRACT

A 1,2,4-triazole motif was employed as a bioisostere for the ester commonly used in muscarinic antagonists, and subsequent integrative conjugation to a β_2 agonist quinolinone furnished a new class of bifunctional MABAs for the treatment of COPD. Medicinal chemistry optimization using the principles of 'inhalation by design' furnished a clinical candidate with desirable pharmacological, pharmacokinetic and biopharmaceutical properties.

© 2015 Elsevier Ltd. All rights reserved.

Chronic obstructive pulmonary disease (COPD) is a leading cause of morbidity and mortality worldwide, and the chronic inflammation associated with the disease leads to emphysema and bronchiolitis.¹ Long-acting β_2 -adrenoceptor agonists (LABAs) and long-acting muscarinic receptor antagonists (LAMAs) form the basis of existing bronchodilator pharmacological treatment.² It has also been shown that bifunctional agents that possess dual pharmacology muscarinic antagonist and β_2 agonist properties (so-called MABAs) can achieve greater efficacy than single bronchodilator modalities alone.³ Triple therapy for COPD, consisting of an anti-inflammatory inhaled corticosteroid (ICS) combined with a LABA and LAMA, will likely provide optimal therapeutic efficacy, particularly for those with concomitant asthma, and an opportunity to address the flare associated with exacerbations.^{1,4,5} However, there are significant technical hurdles to combine three separate drugs in a single inhaler, and therefore the combination of two drugs, a MABA and an ICS would provide substantially simpler opportunities for triple therapy.^{6,7}

We, and others, have described the design and development of dual pharmacology MABAs for the treatment of COPD, with a view to their eventual combination with ICS agents to enable the triple therapy concept (see for example those from Theravance and Pfizer in Figure 1).^{8–11} Here we present the design of a 1,2,4-triazole muscarinic antagonist template which enabled the creation of novel bifunctional MABAs, culminating in the development of a clinical candidate.

A detailed description of the design of the triazole-containing muscarinic antagonist series will appear elsewhere. Briefly, an investigation into novel heterocyclic replacements of the ester linkages often seen in antimuscarinic templates, such as ipratropium, tiotropium and enipiperate,¹² provided the 1,2,4-triazole isostere as an effective mimic that retained the desired pharmacology (Fig. 2 and Table 1—in fact, triazole **1** was more potent than the parent ester enipiperate).¹³ The syntheses of all triazole muscarinic antagonists and MABAs in this manuscript were described previously.¹⁴ Other groups have also reported alternative heterocyclic replacements in the development of novel antimuscarinic agents and MABAs.^{8,9}

* Corresponding author. Tel.: +1 617 665 5631.

E-mail address: lyn.jones@pfizer.com (L.H. Jones).

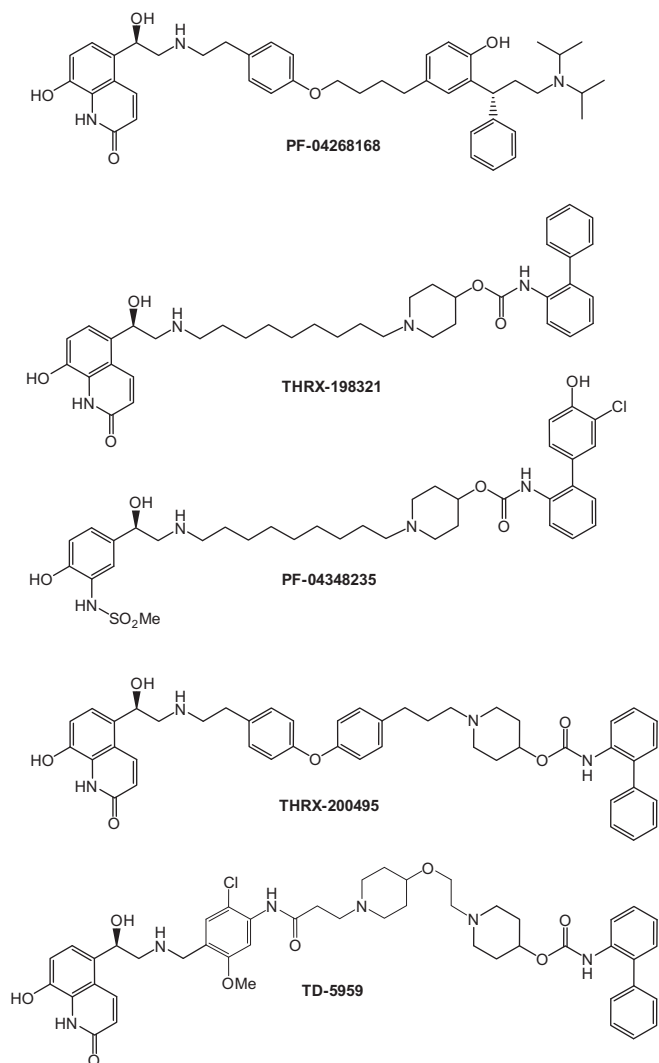


Figure 1. Known dual pharmacology MABA bronchodilators from Pfizer (PF-04268168 and PF-04348235) and Theravance (THR-198321, THR-200495 and TD-5959).

Piperidine was chosen as the motif bearing the key antimuscarinic pharmacophoric nitrogen as it appeared in many MABA templates previously and our own analysis showed that more synthetically complex replacements provided no significant improvements in potency, at least in the biaryl carbamate series.¹⁵ Saturation of one of the benzene rings to a cyclohexane had been shown to improve the potency of other antimuscarinic series,^{16,17} and although there appeared to be little effect in the case of racemic triazole **2** (Fig. 2 and Table 1), we decided that the commensurate increase in lipophilicity of this transformation may positively modulate the pharmacodynamics and pharmacokinetics of a MABA containing this motif (see below).

Next, we conjugated the triazole antimuscarinic motifs to the precedented quinolinone β_2 agonist head group to create novel MABAs. The quinolinone agonist trigger was chosen due to its use in several MABA series previously (THR-198321 for example), and its propensity for glucuronidative phase II metabolism via phenol glycosylation, that can mitigate potential issues for drug-drug interactions (DDIs).¹⁵ We initially chose the C9-linker to conjugate the β_2 and M3 motifs (due to the potential multivalent effects of the resultant MABA¹⁸ and from precedence in our own work)¹⁶ to yield **3** (Table 1). Although **3** possessed adequate β_2 and M3

cell-based activity, the kinetics of pharmacological duration against the M3 receptor (using tritiated *N*-methyl scopolamine in a dilution-based methodology described previously)^{19,20} were relatively poor. Additionally, the metabolic stability of **3** was rather high (as assessed in human liver microsomes, HLM) and there was no evidence of glucuronidation (assessed in HLM in the absence of NADPH and the presence of microsomal activator Brij58 and UDPGA).²¹ The polarity of the triazole ring imparts higher hydrophilicity to the resulting conjugate, which likely drives these observations (cf. *cLogP* of PF-04268168 and PF-04348235 to **3**, Table 1).

The benzene-diethylamine linker was also used to conjugate the β_2 and M3 head groups (precedence exists for this linker in biaryl carbamate MABAs)⁸ to furnish **4**. Unfortunately, this modification had a detrimental effect on the primary pharmacology, although surprisingly, the HLM turnover was higher, even though the molecule was more polar than **3**.

The cyclohexyl-containing triazole MABA **5** was prepared as an epimeric mixture to ascertain the effect of saturating one of the benzene rings in the antimuscarinic pharmacophore.¹⁴ The resulting increase in lipophilicity likely caused the higher metabolic turnover, and adequate primary pharmacology for both β_2 and M3 components was attained. As a result of these preliminary results, the racemic precursor was resolved to enable preparation of the single active enantiomer, and subsequent conjugation yielded **6** and **7**. Both MABAs possessed good primary pharmacology, kinetics and high metabolic turnover in HLM (Table 1). Interestingly, the benzene-diethylamino-linked MABA **7** demonstrated higher glucuronidation than **6**, and therefore this congener (PF-04810097) was chosen for further in vivo and ex vivo profiling. The simultaneous optimization of dual pharmacology and phase I plus II metabolism is a feature of our medicinal chemistry program that differentiates this work from previous MABA drug discovery.¹¹

As found for many other antimuscarinic templates, PF-04810097 exhibited non-selective muscarinic receptor antagonist activity (K_i M1, M2, M3, M4, M5 = 0.16, 0.14, 0.29, 0.35, 1.1 nM, respectively). The M3 off rate of PF-04810097 was relatively slower than ipratropium ($T_{1/2}$ <15 min) but significantly faster than tiotropium (>1372 min) (we had previously shown that a *cLogP* >5.5 for MABAs was required for long offset kinetics).¹⁹ We also observed a mismatch between M3 offset kinetics and antimuscarinic duration of action in the ex vivo guinea pig trachea (GPT) assay in another MABA series,¹⁶ and we were therefore keen to explore the GPT efficacy and duration of PF-04810097 (Table 2).

PF-04810097 produced a concentration-related and potent inhibition of the GPT contraction induced by electric field stimulation, which captures both β_2 and M3 axes. The β_2 antagonist propranolol was then used to delineate the M3 component of bronchodilation, and PF-04810097 retained excellent potency. The duration of action (DoA—the time taken for the EFS response to recover by 25% of the inhibition induced, $T_{25\%}$) was impressive, both in the presence and absence of propranolol. The apparent mismatch with the M3 offset kinetics suggests an alternative mechanism at play in the tissue assay, although further work is warranted to fully explain these observations (a similar effect was reported recently for another MABA¹¹). PF-04810097 was also a potent inhibitor of histamine induced contractions of the isolated GPT preparation (Table 2), which is indicative of β_2 efficacy only, as previously described.¹⁹

PF-04810097 was also assessed for its ability to inhibit methacholine-induced bronchoconstriction in the conscious dog model via intratracheal administration in a micelle solution. PF-04810097 was a potent and long lasting inhibitor of bronchoconstriction in the dog (the potency for PF-04810097 was comparable to other agents such as ipratropium and

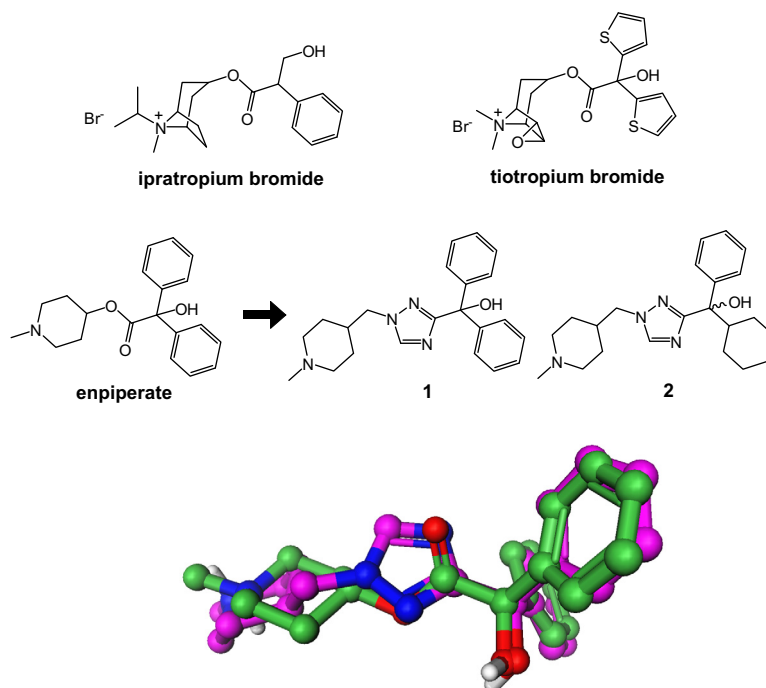
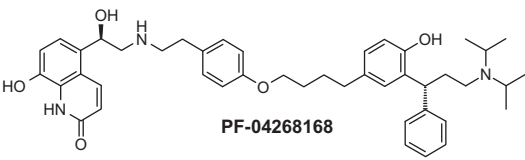
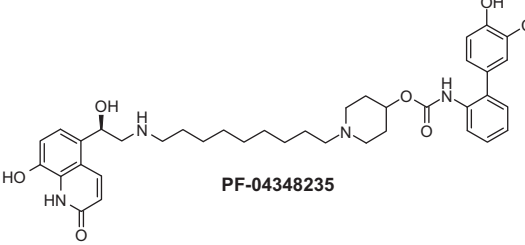
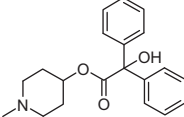
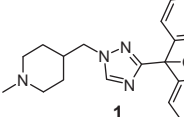
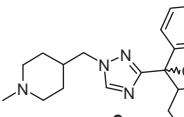


Figure 2. Derivation of 1,2,4-triazole template from the ester-containing antimuscarinics (exemplified by enpipate). Manual overlay of energy-minimized structures of enpipate (green) and triazole **1** (magenta) illustrating colocalization of hydrogen bonding groups, benzene rings and the basic nitrogen atoms.

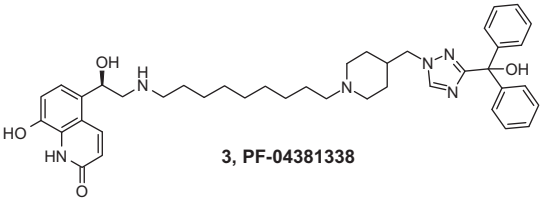
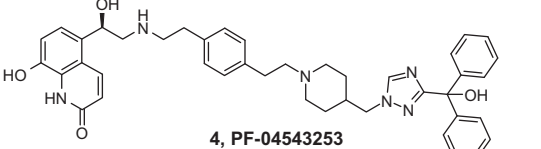
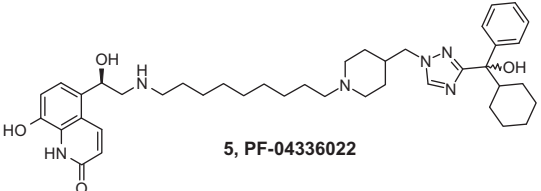
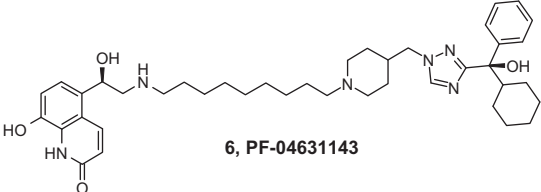
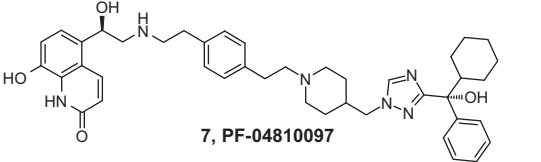
Table 1

In vitro pharmacological and metabolic profiles of PF-04268168, PF-04348235, enpipate and 1,2,4-triazoles^a

Compound	β_2 EC ₅₀ ^b (nM)	β_2 fold shift ^b	M3 K _i (nM)	M3 offset ^c (min)	HLM ^d (μ l/min/mg)	Glucuronidation ^e (μ l/min/mg)	cLogP
 PF-04268168	2.4	1.1	0.31	>1200	74	<3	6.6
 PF-04348235	3.7	1.5	0.73	117	23	24	5.3
 enpipate	n/a	n/a	1.1	nd	nd	nd	2.5
 1	n/a	n/a	0.34	nd	nd	nd	1.2
 2	n/a	n/a	1.1	nd	nd	nd	2.8

(continued on next page)

Table 1 (continued)

Compound	β_2 EC ₅₀ ^b (nM)	β_2 fold shift ^b	M3 K _i (nM)	M3 offset ^c (min)	HLM ^d (μ l/min/mg)	Glucuronidation ^e (μ l/min/mg)	cLogP
 3, PF-04381338	13	3.5	3.7	<15	18	<3	3.7
 4, PF-04543253	116	6.4	18	nd	47	<3	2.6
 5, PF-04336022	21	1.5	7.7	491	160	3.2	4.8
 6, PF-04631143	14	1.2	3.7	278	133	4	4.8
 7, PF-04810097	20.9	2.1	0.29	<100	130	9	3.7

^a nd = not determined; n/a = not applicable.^b Washed and unwashed agonist potency of compounds at the β_2 adrenoceptor, by measuring their ability to stimulate intracellular cAMP production in CHO-h β_2 cells.^c offset kinetics from human cloned M3 receptor using [³H] N-methyl scopolamine (dilution method).^d Clearance values in human liver microsomes.^e Glucuronidation rate assessed in HLM (–NADPH, +Brij, +UDPGA).

Table 2

Ex vivo and in vivo pharmacological profiles of lead triazole MABA PF-04810097, salmeterol and ipratropium^a

	PF-04810097	Salmeterol	Ipratropium
GPT EFS EC ₅₀ ^b (nM)	11.5	6.9	1.2
GPT EFS duration T _{25%} ^b (h)	>16	8.2	2.6
GPT EFS + propranolol EC ₅₀ ^c (nM)	10.2	NA	NA
GPT EFS + propranolol duration ^c (h)	>12.4	NA	NA
GPT histamine EC ₅₀ ^d (nM)	12.9	2.7	NA
Conscious dog ID ₅₀ ^e (μ g)	56	14	11
Conscious dog CV TI ^f	20-fold	7-fold	No effect
Conscious dog duration ^g (h)	16	10	<4

^a All data are geometric means with 95% CI, at least $n = 4$.^b GPT = Guinea pig trachea. EFS = Electric field stimulation. Potency and duration for β_2 and M3 components of bronchodilation. Submaximal concentration used for the duration is that which gives 70% inhibition of the EFS response.^c Potency and duration for M3 component of bronchodilation.^d Potency for β_2 component of bronchodilation.^e Bronchodilator effect in methacholine-induced bronchoconstriction model in conscious dogs.^f Therapeutic index over heart rate and contractility in the methacholine-induced bronchoconstriction model in conscious dogs.^g Duration of action in the methacholine-induced bronchoconstriction model in conscious dogs at 30 μ g dose.

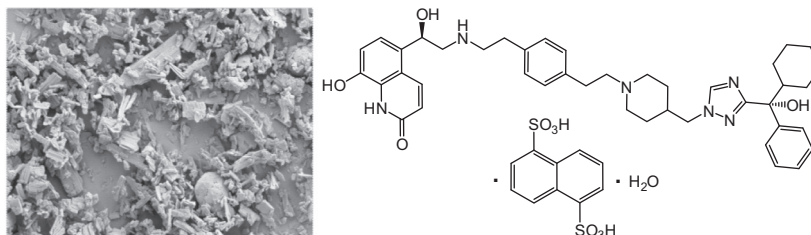


Figure 3. Scanning electron micrograph of freshly micronized PF-04810097 naphthalene 1,5-disulfonate hydrate showing very fine particles, typically less than 2 μm in diameter.

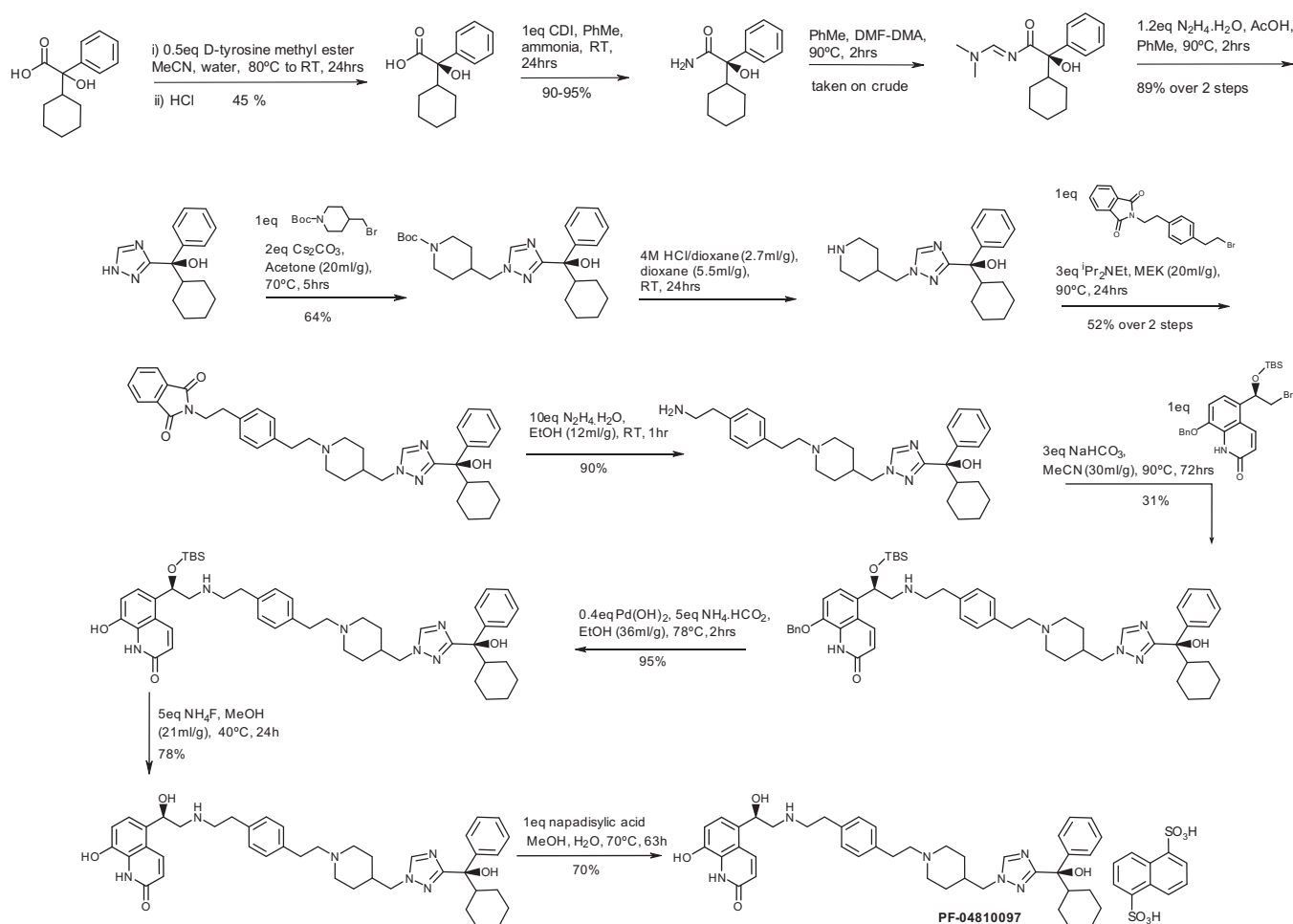


Figure 4. The discovery synthetic route to PF-04810097.

salmeterol in the same model (ID_{50} 11 and 14 μg respectively, Table 2). PF-04810097 also displayed a three-fold superior therapeutic index for heart rate and contractility over salmeterol in this model. In anesthetized rabbits, PF-04810097 did not cause activation of A δ fibers from the tracheobronchial tree, suggesting that it would be unlikely to cause cough in humans following inhaled administration.²² Also from a safety perspective, PF-04810097 was found to be clean in genetic toxicity screening (AMES and in vitro micronucleus).

PF-04810097 exhibited a moderate plasma clearance (22 and 11 mL/min/Kg in rat and dog respectively) and a short-to-moderate half life (1.7 and 4 h). Following oral solution administration to rats (2 mg/Kg), bioavailability was determined to be low (<5%) as

desired (concentrations were below the lower limit of detection) thus minimizing potential risks from systemic exposure. The routes of metabolism were determined in HLM and preclinical species (rat and dog), which were consistent with N-dealkylation at the piperidine and secondary amine groups, and a glucuronide conjugate of the β_2 phenol was isolated in human hepatocytes as predicted. Although further work is required to fully profile the pharmacology of these metabolites, their very low predicted circulating levels, due to inhaled dosing and poor oral bioavailability of the parent, mitigate potential issues arising from active metabolites.

A desirable solid form for inhalation dosing in a dry powder inhaler (DPI) is extremely important in the development of a viable bronchodilator, especially if the ultimate aim for a MABA is to

combine it with an ICS. As other related MABAs had been crystallized previously as their naphthalene 1,5-disulfonate salts using Armstrong's acid,¹⁵ this was also attempted with PF-04810097. Pleasingly, PF-04810097 was crystallized as the naphthalene 1,5-disulfonate (melting point 257 °C), so enabling further development (Fig. 3). From dynamic vapor sorption and thermal analysis data, the solid form appeared to be hydrated and the crystal did not change form upon dehydration and subsequent re-hydration. Crystalline feed material was micronized at an air jet mill pressure of 5 bar (in a MCOne® spiral jet mill) and the appearance of the micronized particles did not change following two weeks exposure to 75% relative humidity at 40 °C (Fig. 3). Jet milled material was blended (1% w/w) with lactose (a common carrier excipient used in DPIs) and accelerated stability testing at 70 °C, 75% relative humidity for one week showed that no single impurity increased to beyond the 0.3% level. The efficacious dose projection of PF-04810097 naphthalene 1,5-disulfonate hydrate (based on comparative data for the clinical agents salmeterol and ipratropium in the well-studied conscious dog model) is 100–300 µg *bid*, 400–1000 µg *qd* nominal dose, corresponding to a lung dose of ~20–60 µg *bid* or ~80–200 µg *qd*, assuming 20% aerosolisation efficiency from the inhaler device. PF-04810097 was therefore nominated as a clinical candidate for the treatment of COPD.

In conclusion, the 1,2,4-triazole motif was employed as a bioisostere for the ester commonly used in muscarinic antagonists, and subsequent conjugation to a β_2 agonist quinolinone furnished a new class of bifunctional MABAs. Further elaboration and development of this series, including a detailed description of the pharmacology and pharmacokinetics of PF-04810097, and its optimized synthetic route (based on the discovery route described in Fig. 4) to provide kilogram quantities of material, will appear elsewhere.

Acknowledgement

We thank Kevin Dack, Alan Stobie and Mark Bunnage for useful discussions.

References and notes

- Vestbo, J.; Hurd, S. S.; Agusti, A. G.; Jones, P. W.; Vogelmeier, C.; Anzueto, A.; Barnes, P. J.; Fabbri, L. M.; Martinez, F. J.; Nishimura, M.; Stockley, R. A.; Sin, D. D.; Rodriguez-Roisin, R. *Am. J. Respir. Crit. Care Med.* **2013**, 187, 347.
- Montuschi, P.; Ciabattoni, G. *J. Med. Chem.* **2015**, 58, 4131.
- Cazzola, M.; Lopez-Campos, J. L.; Puente-Maestu, L. *Eur. Respir. J.* **2013**, 42, 885.
- Welte, T.; Miravittles, M.; Hernandez, P.; Eriksson, G.; Peterson, S.; Polanowski, T.; Kessler, R. *Am. J. Respir. Crit. Care Med.* **2009**, 180, 741.
- Singh, D.; Brooks, J.; Hagan, G.; Cahn, A.; O'Connor, B. J. *Thorax* **2008**, 63, 592.
- Fuso, L.; Mores, N.; Valente, S.; Malerba, M.; Montuschi, P. *Curr. Med. Chem.* **2013**, 20, 1477.
- Montuschi, P.; Macagno, F.; Valente, S.; Fuso, L. *Curr. Med. Chem.* **2013**, 20, 1464.
- Hughes, A. D.; Jones, L. H. *Future Med. Chem.* **2011**, 3, 1585.
- Hughes, A. D.; McNamara, A.; Steinfeld, T. *Prog. Med. Chem.* **2012**, 51, 71.
- McNamara, A.; Steinfeld, T.; Pulido-Rios, M. T.; Stangeland, E.; Hegde, S. S.; Mammen, M.; Martin, W. J. *Pulm. Pharmacol. Ther.* **2012**, 25, 357.
- Hughes, A. D.; Chen, Y.; Hegde, S. S.; Jasper, J. R.; Jaw-Tsai, S.; Lee, T. W.; McNamara, A.; Pulido-Rios, M. T.; Steinfeld, T.; Mammen, M. *J. Med. Chem.* **2015**, 58, 2609.
- Xu, R.; Sim, M.-K.; Go, M.-L. *Eur. J. Pharm. Sci.* **1999**, 8, 39.
- Yang, R.-S.; Hu, G.-Q.; Huang, W.-L. *Huaxue Shiji* **2008**, 30, 8.
- Jones, L. H.; Roberts, D. F.; Strang, R. S. 2010; Vol. WO2010004517.
- Hilton, L.; Osborne, R.; Kenyon, A. S.; Baldock, H.; Bunnage, M. E.; Burrows, J.; Clarke, N.; Coghlan, M.; Entwistle, D.; Fairman, D.; Feeder, N.; James, K.; Jones, R. M.; Laouar, N.; Lunn, G.; Marshall, S.; Newman, S. D.; Patel, S.; Selby, M. D.; Spence, F.; Stuart, E. F.; Summerhill, S.; Trevethick, M. A.; Wright, K. N.; Yeadon, M.; Price, D. A.; Jones, L. H. *Med. Chem. Commun.* **2011**, 2, 870.
- Osborne, R.; Clarke, N.; Glossop, P.; Kenyon, A. S.; Liu, H.; Patel, S.; Summerhill, S.; Jones, L. H. *J. Med. Chem.* **2011**, 54, 6998.
- Carter, J. P.; Noronha-Blob, L.; Audia, V. H.; Dupont, A. C.; McPherson, D. W.; Natalie, K. J., Jr.; Rzeszutowski, W. J.; Spagnuolo, C. J.; Waid, P. P.; Kaiser, C. J. *Med. Chem.* **1991**, 34, 3065.
- Steinfeld, T.; Hughes, A. D.; Klein, U.; Smith, J.; Mammen, M. *Mol. Pharmacol.* **2011**, 79, 389.
- Jones, L. H.; Baldock, H.; Bunnage, M. E.; Burrows, J.; Clarke, N.; Coghlan, M.; Entwistle, D.; Fairman, D.; Feeder, N.; Fulton, C.; Hilton, L.; James, K.; Jones, R. M.; Kenyon, A. S.; Marshall, S.; Newman, S. D.; Osborne, R.; Patel, S.; Selby, M. D.; Stuart, E. F.; Trevethick, M. A.; Wright, K. N.; Price, D. A. *Bioorg. Med. Chem. Lett.* **2011**, 21, 2759.
- Watson, J.; Strawbridge, M.; Brown, R.; Company, K.; Coghlan, M.; Trevethick, M. A. *Fund. Clin. Pharm.* **2008**, 22, 69.
- Trubetskoy, O.; Finel, M.; Trubetskoy, V. J. *Pharm. Pharmacol.* **2008**, 60, 1061.
- Sladen, L.; Clarke, N.; Perros-Huguet, C.; Yeadon, M. *Am. J. Respir. Crit. Care Med.* **2011**, 183, A3099 (poster).